Nanoscience and
Nanotechnology Letters
Vol. 7, 817–821, 2015

Optical Properties of Arsenic-Doped MgZnO Films Treated by Thermal Annealing

X. Gao[1], S. Xing[2,*], J. L. Tang[1,*], D. Fang[1], X. Fang[1], S. P. Wang[3], H. F. Zhao[3], F. Fang[4], J. H. Li[1], X. Y. Chu[1], F. Wang[1], X. H. Wang[1], and Z. P. Wei[1,*]

[1] *State Key Laboratory of High Power Semiconductor Laser, School of Science, Changchun University of Science and Technology, Changchun 130022, People's Republic of China*
[2] *Globalfoundries Singapore Pte. Ltd, 60 Woodlands Industrial Park D Street 2, Singapore 738406*
[3] *Changchun Institute of Optics, Fine Mechanics and Physics, Chinese Academy of Science, Changchun, 130033, People's Republic of China*
[4] *Nanchang University, Jiangxi, Nanchang, 330047, People's Republic of China*

Arsenic-doped MgZnO films were grown using plasma-assisted molecular beam epitaxy (MBE). The incorporation of arsenic was achieved by annealing the MgZnO films that were grown on GaAs (100) substrate. The films did not undergo phase separation and exhibited a high C-axis orientation, as determined using X-ray diffraction. The photoluminescence spectra of the samples annealed at 550 °C revealed an acceptable bound exciton peak at 3.400 eV when excited using a He–Cd laser (325 nm) at 10 K. The photoluminescence of the as-grown samples revealed a bound exciton peak at 3.410 eV when excited using the same conditions. It confirms that arsenic-doped MgZnO films were obtained and that the donor defects in the MgZnO films were effectively suppressed following diffusion of the arsenic.

Keywords: MgZnO, As Doping, Photoluminescence, Molecular Beam Epitaxy.

1. INTRODUCTION

ZnO is a direct band gap semiconductor material with a wide-band gap value of 3.37 eV. This makes ZnO an attractive material for ultraviolet (UV) light emitters and detectors.[1–10] MgZnO is an important member of ZnO, besides, the band gap energy of MgZnO could be adjusted via varying the Mg composition.[11,12] Doping is widely employed to tailor the band structures of bulk and nanoscale materials to create multifunctional materials and devices.[13–22] However, *p*-type doping remains a major challenge for both ZnO and MgZnO.[23–29] Group V elements are considered as the reliable doping source to achieve *p*-type doping. For ZnO, arsenic (As) doping has been confirmed as a feasible method.[30–37] As-doping has been achieved by growing ZnO films, or nanowires, on GaAs substrates. Alternatively, GaAs wafers can be attached onto the surface of ZnO using thermal diffusion. The post-annealing process causes the As ions to diffuse into ZnO, yielding a *p*-type ZnO material.[30]

In this paper, we report the successful doping of MgZnO films with As by annealing films that were grown on GaAs (100) substrates. The photoluminescence (PL) of the films was examined and confirmed that the films exhibited acceptor behavior. High-quality MgZnO films were grown on semi-insulating GaAs (100) substrates using plasma-assisted molecular beam epitaxy (P-MBE).[31,32] The as-grown films were annealed to induce diffusion of As into the MgZnO layer. The electrical and optical properties of the samples were dependent upon the amount of time that the samples were annealed.

The PL spectra collected at 10 K exhibited an acceptor bound exciton (A^0X) peak near 3.400 eV, while the emission spectra, collected at 40 K, exhibited a free exciton (FX) peak at 3.420 eV. These spectroscopic behaviors are similar to those observed in *p*-type ZnO films doped with N. Undoped ZnO is dominated by a donor bound exciton (D^0X) peak and an FX peak.[33–40] These results confirmed that As-doped MgZnO films were obtained when annealed under optimum conditions.

2. EXPERIMENTAL DETAILS

MgZnO thin films (sample A) were grown on GaAs (100) substrates using P-MBE. The substrates were subjected

*Authors to whom correspondence should be addressed.

 1941-4900/2015/7/817/005 doi:10.1166/nnl.2015.2041

to ultrasonication in ethanol to remove surface contamination then subsequently etched in a H_2SO_4:H_2O_2:H_2O (3:1:1) solution for 5 min. The samples were then rinsed with deionized water (18.2 MΩ cm^{-1}) and dried under a flow of high purity nitrogen. To obtain a clean surface, the substrates were treated in vacuum ($\leq 1 \times 10^{-7}$ Pa) at 550 °C for 30 min in an MBE chamber (a preparation chamber for *in-situ* processes such as degassing). A Knudsen effusion cell was used to evaporate elemental zinc with 99.9999% purity and elemental magnesium with 99.999% purity. The gas sources were activated by an Oxford Applied Research Model HD25 radio frequency (RF) plasma source (13.56 MHz) atomic source. An electrostatic ion trap (EIT) operated at 500 V was used to separate the activated ions and atoms during the growth process. The Zn and Mg beam pressure partial pressure were fixed at 4×10^{-4} Pa and 4×10^{-6} Pa, respectively. The temperature in the growth chamber was maintained at 245 °C. High-purity O_2 gas was controlled using mass flow controllers and was injected into the RF plasma source. The plasma power was 300 W. The growth temperature was 550 °C. The thickness of the MgZnO films was approximately 400 nm, as determined using scanning electron microscopy (SEM).[41] The Energy Dispersive X-ray detector (EDX) results were measured in SEM mode. To ensure the diffusion of As into the films, the as-grown samples were annealed in the Oxygen atmosphere at 550 °C for 0.5 and 1 h (samples B and C, respectively).

Crystal structures of the as-grown samples were characterized using X-ray diffraction (XRD, D/max-RA) with Cu-Ka radiation ($\lambda = 1.5406$ Å). A JY-63 spectrometer with a He–Cd laser excitation source (325 nm) was used to measure the PL spectra of the samples. The electronic properties of the films were measured using an HL5500PC system made by the Bio-Rad Corporation.

3. RESULTS AND DISCUSSION

X-ray diffraction (XRD) pattern of the as-grown MgZnO film (sample A) is shown in Figure 1. The strong (002) peak revealed that the MgZnO film had a single-phase hexagonal wurtzite structure with the preferred orientation of the *C*-axis perpendicular to the substrate surface. There was no indication of any significant formation of a separated MgO phase. Compared with undoped ZnO, the (002) peaks exhibited a shift from 34.42° to 34.54°, indicating that Mg was indeed introduced into the ZnO (Inset of Fig. 1).[12]

To verify the presence of As in the MgZnO films after annealing, EDX spectra were measured at different positions of both the as-grown (sample A) and the annealed (sample C) films (Fig. 2). The As concentration in the films reached a maximum value within the GaAs substrate for both samples (Fig. 2(b)). However, the concentration of As was clearly enhanced in the annealed MgZnO film when compared with that of the as-grown film. Some

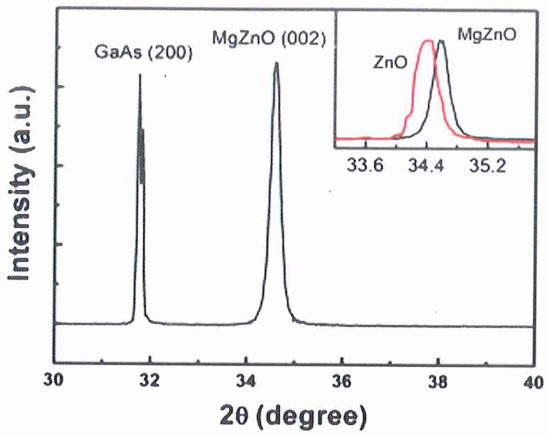

Fig. 1. XRD patterns of the as-grown MgZnO film (sample A). Inset shows an overlay of the XRD spectra of ZnO and the as-grown MgZnO film (sample A).

diffusion of Zn from the MgZnO film into the GaAs substrate was also observed.

Hall-effect measurements were used to determine the electrical properties of the As-doped MgZnO films. The results are summarized in Table I. The carrier mobility of the as-grown films increased when annealed at 550 °C for 0.5 h; however, the carrier density decreased. These effects are associated with dopant-induced defects. When As is doped into the MgZnO after annealing, the oxygen atom will be substituted, the doped alloy form a *p*-type semiconductor.[28] Therefore, as the concentration of As is increased, defects related to acceptor materials will also increase.

To confirm that acceptor-related defects were formed in the films following doping with As, PL spectrometry

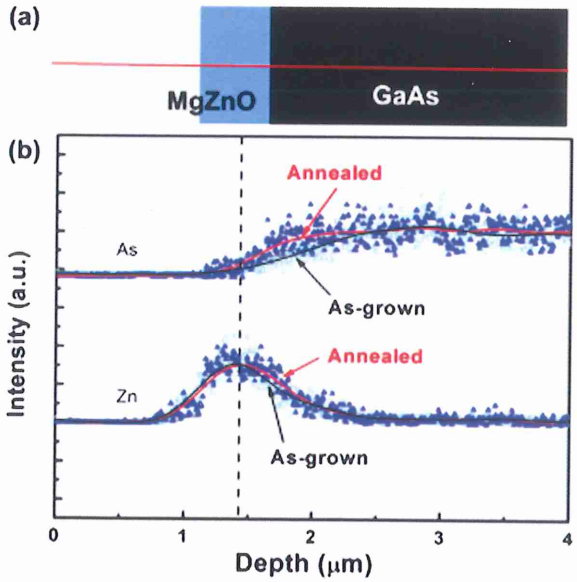

Fig. 2. (a) Scheme of the MgZnO film on a GaAs substrate. (b) The EDX patterns of the as-grown MgZnO film (sample A) and the annealed MgZnO film (sample C).

Table I. Hall-effect measurements data summary of the as-grown MgZnO film (sample A) and the annealed MgZnO films (samples B and C).

	As-grown (Sample A)	550 °C and 0.5 h (Sample B)	550 °C and 1 h (Sample C)
Conduction type	*n*	*n*	High resistivity
Mobility ($cm^2\ V^{-1}\ s^{-1}$)	1.1	2.5	–
Carrier density (cm^{-3})	5.4×10^{17}	2.6×10^{16}	–

was used to investigate the optical properties of the films. PL spectra of undoped ZnO, the as-grown MgZnO film, and the annealed MgZnO film collected at ambient temperature are shown in Figure 3. The undoped ZnO exhibited a strong UV emission at 3.302 eV, which corresponds to the near-band-edge emission of ZnO. Compared with the undoped ZnO sample, the dominant emission peak for the as-grown MgZnO film showed a blue shift from 3.302 to 3.366 eV (Fig. 3), which may be associated with donor-bound exciton emission (i.e., broadening of the band-gap).[40] The emission peak at 3.302 eV was also be observed from the as-grown and annealing MgZnO films. This was ascribed to emission from ZnO. Moreover, the peak intensities of the annealed samples increased with increasing annealing times.

PL spectra of the as-grown MgZnO film (sample A) collected at different temperatures are shown in Figure 4(a). An overlay of the PL spectra of the as-grown film and the annealed film (sample C), collected at 12 K, is shown in Figure 4(b). The main emission peak located at 3.413 eV is caused by emission from excitons bound to neutral donors, while the peak at 3.423 eV is ascribed to emission from free excitons (Fig. 4(a)).[42] As the temperature at which the spectra were collected was increased, the intensity of the D^0X emission became weaker while the FX emission became stronger. Following annealing in the Oxygen atmosphere for 1 h at 550 °C (sample C), the emission maxima was located at 3.400 eV, while that of the as-grown sample

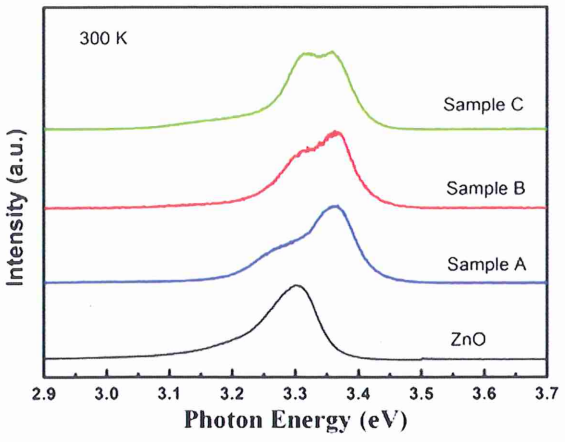

Fig. 3. Ambient temperature PL spectra of undoped ZnO, the as-grown MgZnO film (sample A), and the annealed MgZnO films (Samples B and C).

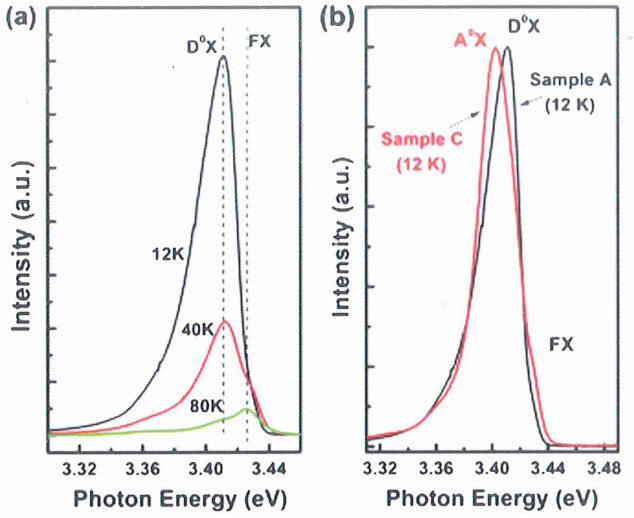

Fig. 4. (a) PL spectra of the as-grown MgZnO film (sample A), recorded at different temperatures. (b) PL spectra of the as-grown MgZnO film (sample A) and the annealed MgZnO film (sample C) recorded at 12 K.

exhibited a bound exciton peak at 3.413 eV (Fig. 4(b)). To the best of our knowledge, As acts as an acceptor in ZnO. Thus, the main emission peak observed from sample C can be attributed primarily to the emission from acceptor-bound excitons.[43] Accordingly, the donor defects should be effectively suppressed after annealing. This data are in agreement with the EDX results discussed previously (Fig. 2). This supported the fact that As-doped MgZnO films were obtained.

To investigate the influence of annealing on the optical properties of the MgZnO films, they were annealed for 0.5 h and 1 h. PL spectra of the as-grown MgZnO film (plot A) and the annealed MgZnO films (plot B and C) collected at 80 K are shown in Figure 5(a). The position

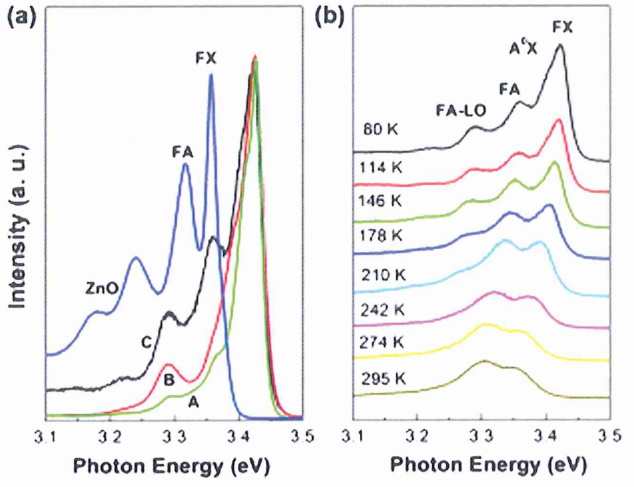

Fig. 5. (a) PL spectra of the as-grown MgZnO film (sample A), the annealed MgZnO films (samples B and C), and annealed ZnO, recorded at 80 K. (b) Temperature-dependent photoluminescence spectra of the annealed MgZnO films.

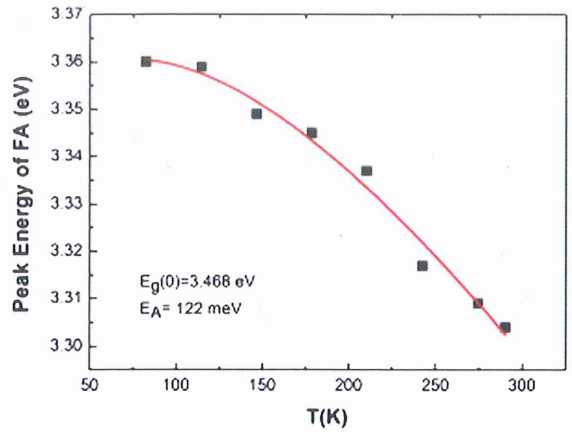

Fig. 6. Plots of the emission energies of the FA peak as a function of temperature.

of main PL peak did not change after annealing. However, the lower-energy shoulder exhibited a monotonic increase with longer annealing times. The peak of as-grown sample located at 3.360 eV can be attributed to FA emission. The intensity of this emission increased with longer annealing times and was strongest following annealing for 1 h (sample C). To understand these observations, the spectra of the annealed MgZnO film and annealed ZnO were compared (Fig. 5(a)). The low-energy shoulder observed in the ZnO emission was caused by Zn-related defects. This implied that Zn-related defects were decreasing as the annealed time increased.[44,45] The emission of the annealed MgZnO films exhibited a blue-shift, which was caused by doping ZnO with Mg. The emission at 3.420 eV was caused by an acceptor-bound exciton in MgZnO (shown in Fig. 5(a) line A, B and C). A shoulder on the FX emission was observed, which was ascribed to an A^0X emission. To further investigate the details of this shoulder emission, the A^0X peak plot of the annealed MgZnO film (sample C) was collected at a range of temperatures, shown in Figure 6. As the temperature was increased, the emission exhibited a red shift, which confirmed that the band gap was temperature dependent.[46,50] The intensity of the A^0X emission decreased as the temperature at which the spectra was recorded was increased. This confirmed that the peak was caused by an A^0X emission. We have demonstrated that the donor-bound emission was suppressed following diffusion of As in the MgZnO films.

To confirm the dissociation processes of the exciton complexes, the energy dispersion of PL lines with the variation of temperature (Fig. 6). The binding energy of the FA state was estimated to be 122 meV from curve fitting of the plot.[45] The FA peak belongs to the As acceptor level in the MgZnO films.

4. CONCLUSIONS

Arsenic-doped MgZnO films with a wurtzite structure were obtained through plasma-assisted molecular-beam epitaxy. The crystalline quality of MgZnO films was improved following annealing. The A^0X, FA emission related with As acceptor in the PL measurements we observed. Therefore, the surface donor defects can be effectively suppressed when MgZnO films are doped with As. The As acceptor level in the MgZnO films was estimated to be 122 meV.

Acknowledgment: This work is supported by the National Natural Science Foundation of China (61204065, 61205193, 61307045, 61404009, 61474010, 61574022, 61504012, 11404219, 11404161, 11574130 and 11204224), the Foundation of State Key Laboratory of High Power Semiconductor Lasers, the Developing Project of Science and Technology of Jilin Province (20130101026JC), the Project of Jilin Province Development and Reform (2014Y110), the Project of Education Department of Jilin Province (2015(70)) and the Project of Changchun Science and Technology (14KG018).

References and Notes

1. Z. P. Wei, Y. M. Lu, D. Z. Shen, Z. Z. Zhang, B. Yao, B. H. Li, J. Y. Zhang, D. X. Zhao, X. W. Fan, and Z. K. Tang, *Appl. Phys. Lett.* 90, 042113 (**2007**).
2. G. Z. Xing, C.-J. Cheng, M. He, S. Li, and T. Wu, *Appl. Phys. Lett.* 103, 022402 (**2013**).
3. H. Zhu, C. X. Shan, J. Y. Zhang, Z. Z. Zhang, B. H. Li, D. X. Zhao, B. Yao, D. Z. Shen, X. W. Fan, Z. K. Tang, X. H. Hou, and K. L. Choy, *Adv. Mater.* 22, 1877 (**2010**).
4. M. Sun, Q. F. Zhang, and J. L. Wei, *J. Phys. D: Appl. Phys.* 40, 3798 (**2007**).
5. J. J. Lee, G. Z. Xing, J. B. Yi, T. Chen, M. Ionescu, and S. Li, *Appl. Phys. Lett.* 104, 10 (**2014**).
6. P. K. Shrestha, Y. T. Chun, and D. P. Chu, *Light: Sci. Appl.* 4, e259 (**2015**).
7. D. D. Wang, G. Z. Xing, F. Yan, Y. S. Yan, and S. Li, *Appl. Phys. Lett.* 104, 022412 (**2014**).
8. G. Z. Xing, Y. H. Lu, Y. F. Tian, J. B. Yi, C. C. Lim, Y. F. Li, G. P. Li, D. D. Wang, B. Yao, J. Ding, Y. P. Feng, and T. Wu, *AIP Advances* 1, 022152 (**2011**).
9. G. Z. Xing, D. D. Wang, B. Yao, A. Q. L. FoongNien, and Y. S. Yan, *Chem. Phys. Lett.* 515, 132 (**2011**).
10. Y. Tian, X. Ma, Y. D. S. Li, and D. R. Yang, *Appl. Phys. Lett.* 97, 061111 (**2010**).
11. D. X. Zhao, Y. C. Liu, D. Z. Shen, Y. M. Lu, J. Y. Zhang, and X. W. Fan, *J. Appl. Phys.* 90, 5561 (**2001**).
12. Y. Y. Lai, Y.-P. Lan, and T. C. Lu, *Light: Sci. Appl.* 2, e76 (**2013**).
13. G. H. Kim, L. Shao, K. Zhang, and K. P. Pipe, *Nat. Mater.* 12, 719 (**2013**).
14. V. S. Sergey, C. Mou, E. G. Turitsyna, A. Rozhin, S. K. Turitsyn, and K. Blow, *Light: Sci. Appl.* 3, e131 (**2014**).
15. P. Wang, Y. P. Wang, and L. M. Tong, *Light: Sci. Appl.* 2, e102 (**2013**).
16. G. Z. Xing, J. B. Yi, F. Yan, T. Wu, and S. Li, *Appl. Phys. Lett.* 104, 202411 (**2014**).
17. J. J. Lee, G. Z. Xing, J. B. Yi, T. Chen, S. Li, and M. Ionescu, *Appl. Phys. Lett.* 104, 012405 (**2014**).
18. T. Grossmann, T. Wienhold, U. Bog, T. Beck, C. Friedmann, H. Kalt, and T. Mappes, *Light: Sci. Appl.* 2, e82 (**2013**).
19. D. D.Wang, Q. Chen, G. Z. Xing, J. B. Yi, S. Rahman, J. Ding, J. L. Wang, and T. Wu, *Nano Letters* 12, 3994 (**2014**).

20. E. M. Dianov, *Light: Sci. Appl.* 1, e12 (**2012**).
21. J. Limpert, F. Stutzki, F. Jansen, H.-J. Otto, T. Eidam, C. Jauregui, and A. Tünnermann, *Light: Sci. Appl.* 1, e8 (**2012**).
22. P. Nikitas, N. Papasimakis, S. Thongrattanasiri, N. I. Zheludev, and F. J. García de Abajo, *Light: Sci. Appl.* 2, e78 (**2013**).
23. C. X. Shan, Z. Liu, and S. K. Hark, *Appl. Phys. Lett.* 92, 073103 (**2008**).
24. Z. P. Wei, B. Yao, Z. Z. Zhang, Y. M. Lu, D. Z. Shen, B. H. Li, X. H. Wang, J. Y. Zhang, D. X. Zhao, X. W. Fan, and Z. K. Tang, *Appl. Phys. Lett.* 89, 102104 (**2006**).
25. A. Osinsky, J. W. Dong, M. Z. Kauser, B. Hertog, A. M. Dabiran, P. P. Chow, S. J. Pearton, O. Lopatiuk, and L. Chernyak, *Appl. Phys. Lett.* 85, 4272 (**2004**).
26. G. Coli and K. K. Bajaj, *Appl. Phys. Lett.* 78, 2861 (**2001**).
27. B. P. Zhang, N. T. Binh, K. Wakatsuki, C. Y. Liu, Y. Segawa, and N. Usami, *Appl. Phys. Lett.* 86, 032105 (**2005**).
28. W. J. Fan, J. B. Xia, P. A. Agus, S. T. Tan, S. F. Yu, and X. W. Sun, *Appl. Phys. Lett.* 99, 013702 (**2006**).
29. J. W. Dong, A. Osinsky, B. Hertog, A. M. Dabiran, P. P. Chow, Y. W. Heo, D. P. Norton, and S. J. Pearton, *J. Electr. Mater.* 34, 416 (**2005**).
30. W. Lee, M. C. Jeong, S. W. Joo, and J. M. Myoung, *Nanotechnology* 16, 764 (**2005**).
31. B. Zhang, Z. Wang, S. Brodbeck, C. Schneider, M. Kamp, S. Hofling, and H. Deng, *Light: Sci. Appl.* 3, e135 (**2014**).
32. K. Lee, J. Lee, B. A. Mazor, and S. R. Forrest, *Light: Sci. Appl.* 4, e288 (**2015**).
33. Y. R. Ryu, T. S. Lee, and H. W. White, *Appl. Phys. Lett.* 83, 87 (**2003**).
34. J. Y. Zhang, P. J. Li, H. Sun, X. Shen, T. S. Deng, K. T. Zhu, Q. F. Zhang, and J. L. Wu, *Appl. Phys. Lett.* 93, 021116 (**2008**).
35. S. Limpijumnong, S. B. Zhang, S. H. Wei, and C. H. Park, *Phys. Rev. Lett.* 92, 155504 (**2004**).
36. W. Lee, M. C. Jeong, and J. M. Myoung, *Appl. Phys. Lett.* 85, 6167 (**2004**).
37. Y. R. Ryu, T. S. Lee, J. H. Leem, and H. W. White, *Appl. Phys. Lett.* 83, 4032 (**2003**).
38. H. S. Kang, G. H. Kim, D. L. Kim, H. W. Chang, B. D. Ahn, and S. Y. Lee, *Appl. Phys. Lett.* 89, 181103 (**2006**).
39. H. Guan, X. C. Xia, Y. T. Zhang, F. B. Gao, W. C. Li, G. G. Wu, X. P. Li, and G. T. Du, *J. Phys.: Condens. Matter.* 20, 292202 (**2008**).
40. F. X. Xiu, Z. Yang, L. J. Mandalapu, J. L. Liu, and W. P. Beyermann, *Appl. Phys. Lett.* 88, 052106 (**2006**).
41. X. Gao, J. L. Tang, D. Fang, S. P. Wang, X. H Ma, H. F. Zhao, X. Fang, Y. F. Li, X. H. Wang, Z. K. Xu, and Z. P. Wei, *Nanosci. Nanotechnol. Lett.* 7, 1 (**2015**).
42. X. Fang, J. H. Li, D. X. Zhao, D. Z. Shen, B. H. Li, and X. H. Wang, *J. Phys. Chem. C* 113, 21208 (**2009**).
43. G. Z. Xing, B. Yao, C. X. Cong, T. Yang, Y. P. Xie, B. H. Li, and D. Z. Shen, *J. Alloy Compd.* 457, 36 (**2008**).
44. K. H. Tam, C. K. Cheung, Y. H. Leung, A. B. Djurišić, C. C. Ling, C. D. Beling, S. Fung, W. M. Kwok, W. K. Chan, D. L. Phillips, L. Ding, and W. K. Ge, *J. Phys. Chem. B* 110, 20865 (**2006**).
45. H. Gao, M. Y. Zhou, H. Ji, X. Z. Wang, and Z. G. Zhang, *J. Alloy. Compd.* 464, 234 (**2008**).
46. D. Fang, X. Fang, Y. Li, B. Yao, H. Zhao, Z. Wei, J. Tang, C. Du, J. Li, X. Ma, D. D. Wang, and Y. S. Yan, *Nanosci. Nanotechnol. Lett.* 7, 117 (**2015**).
47. C. X. Shan, Z. Liu, and S. K. Hark, *Appl. Phys. Lett.* 92, 073103 (**2008**).
48. S. Tian, Z. P. Wei, H. F. Zhao, X. Gao, X. Fang, J. L. Tang, and X. H. Ma, *Nanosci. Nanotechnol. Lett.* 5, 1274 (**2013**).
49. X. Fang, J. H. Li, D. X. Zhao, B. H. Li, Z. Z. Zhang, D. Z. Shen, X. H. Wang, and Z. P. Wei, *Thin Solid Films* 518, 5687 (**2010**).
50. S. C. Chen, T. Y. Kuo, W. C. Peng, S. L. Ou, and H. C. Lin, *Nanosci. Nanotechnol. Lett.* 5, 883 (**2013**).

Received: 10 May 2015. Accepted: 15 October 2015.